Absolute calibration of gravitational wave detector using gravity field and photon pressure

Yuki Inoue[a,b], Sadakazu Haino[a], Nobuyuki Kanda[c], Yujiro Ogawa[b], Toshikazu Suzuki,[d], Takayuki Tomaru[b], Takahiro Yamamoto[e], Takaaki Yokozawa[e]

[a]Institute of Physics, Academia Sinica, Nankang, Taipei 11529, Taiwan;
[b]High Energy Accelerator Research Organization, Tsukuba, Ibaraki, 305-0801, Japan;
[c]Department of Physics, Osaka City University, Sumiyoshi, Osaka 558-8585, Japan;
[d]Institute for Cosmic Ray Research, University of Tokyo, Kashiwa, Chiba, 277-8582, Japan;
[e]KAGRA Observatory, Institute for Cosmic Ray Research, University of Tokyo, Hida, Gifu 506-1205, Japan;

ABSTRACT

Absolute calibration of the gravitational wave detectors are an essential to understand the source parameters of the gravitational wave source. The photon calibrator is primary calibrator for calibrating the absolute displacement of the mirror by using the photon pressure. Current limit of the absolute calibration uncertainty is 3 % corresponding to the uncertainty of the absolute laser power measured by standard institute. In order to reduce the uncertainty of the photon calibrator, we propose a use of the gravity field calibrator. The gravity field calibrator can modulate the mirror using the gravity gradient. However, uncertainty of the distance between the test mass and calibrator is one of the serious systematic error of the absolute calibration. To cancel the uncertainty of the distance between mirror and calibrator, we newly propose a use of quadrupole and hexapole mass distribution. This method can be estimated as the distance with ratio of the quadruple and hexapole response. We also estimated the uncertainty of this method. We considered the systemetic error of transfer function and higher order effect of the multipole moment. The estimated precision of absolute calibration is 0.3%, which is 10 times less than that of previous method.

Keywords: Gravitational Wave, KAGRA, LIGO, Virgo, Calibration

1. INTRODUCTION

The discovery of the gravitational wave gave us the new probe for observing our universe.[?] Instruments for measuring the gravitational wave must be designed for sensitivity as well as precision. The typical strain sensitivity of 2nd generation interferometric detectors (IFO), such as Advanced LIGO, Advanced Virgo,[?] and KAGRA,[?,?] are around $10^{-23}/\sqrt{Hz}$. In order to estimate the parameters of gravitational waves, such as masses, spins, redshift and distance, understanding of the systematic and statistical noise sources are critical.

In particular, the uncertainty of the absolute calibration is directly propagate to the estimation error of the distance of the Compact Binary Coalescence. By applying the Neutron star - Neutron star binary and follow up observation, it can give us the new probe for estimation of the Hubble constant.

To reduce the systematic errors of the gravitational wave calibration and reconstruction, we need to calibrate the response of IFO. The first generation of the photon calibrator is developed by the Glasgow. They proposed the modulation method with photon pressure for understanding the response of interferometer. LIGO employ the second generation photon calibrator for the calibration of time-dependent response of IFO.[?] However, it has a challenging issue of the absolute calibration due to the accuracy of the absolute laser power of laser standard between each country. Current uncertainty by measuring in the each standard institute of each country is a few percent.

The dynamic gravity field generator is one of the candidates to be able to solve the uncertainty problem of absolute calibration. The technologies of the system are established and tested in University of Tokyo and Rome

Yuki Inoue: iyuki@post.kek.jp

Table 1. Specification summary of LIGO, Virgo and KAGRA photon calibrator

	KAGRA	advanced LIGO	advanced Virgo
Mirror material	Sapphire	Silica	Silica
Mirror mass	22.89 kg	40 kg	40 kg
Mirror diameter	220 mm	340 mm	350 mm
Mirror thickness	150 mm	200 mm	200 mm
Distance of Pcal from ETM	36 m	8 m	1.5 m
Pcal laser power	20 W	2W	3 W
Pcal laser frequency	1047 nm	1047 nm	1047 nm
Incident angle	0.72 deg	8.75 deg	30 deg

group. Related techniques using gravity field calibrator for the calibration are discussed in Matone et al.[?] It can modulate the test mass using gravity gradient with rotor. The amplitude of displacement of the mirror is determined by masses, distance, frequency, radius, and Gravity constant.

In this paper, we propose how we can achieve sub-percent uncertainty of the calibration. We focus on the combination method of the photon calibrator and gravity field calibrator. In chapter **??**, we explain how to calibrate with photon calibrator. In chapter **??**, we show the principle of multipole moment gravity and modulation method. In section **??**, we show how to calibrate the absolute displacement with Pcal and Gcal. In section **??**, we discuss the systematic error by changing parameters.

2. PHOTON CALIBRATOR

Photon calibrator (Pcal) relies on the photon radiation pressure from the power modulated laser beams reflecting on the test mass to apply periodic force via the recoil of photons.[?] LIGO, Virgo and KAGRA employ the photon calibrator for the calibration of the interferometer response.[?] Each gravitational detectors placed the 1047 nm laser around the end test mass. The displacement of the test mass can be described as

$$x = \frac{P(\omega)\cos\theta}{2c} s(\omega)\left(1 + \frac{M}{I}\vec{a}\cdot\vec{b}\right), \tag{1}$$

where P is absolute laser power, θ is incident angle of the Pcal laser, M is mass of test mass, ω is angular frequency, $\vec{a}$ and $\vec{b}$ are position vector of Pcal laser beams. $I = Mh^2/12 + Mr^2/4$ is inertia, where h and r are thickness and radius of test mass. $s(\omega)$ is transfer function between force and displacements. We can regard the $s(\omega)$ as $1/(M\omega^2)$ above 20 Hz.

The laser power is stabilized less then design sensitivity. The schematic vier of the photon calibrator is shown in Fig. **??**. The stabilized laser is mounted on the transmitter module. The power is monitored by the response of the photo detectors at the transmitter module and receiver module. The uncertainty of displacement corresponds to uncertainty of laser power. The largest relative uncertainty of photon calibrator is that of laser power. LIGO and KAGRA use the working standard to cross-calibrate the relative response of each interferometer. The relative uncertainty of each calibrator is 0.51 %.[?] The second largest relative uncertainty of photon calibrator is optical efficiency of optical path. We calibrate the injected power from outside of the vacuum chamber. We need to estimate the laser power response through the response of photo detector at the outside of vacuum chamber. The measured uncertainty of optical efficiency in LIGO is 0.37 %. For the absolute calibration, the detector, so called Gold standard, is compared with the NIST laser power standard. We send Gold standard to NIST and calibrate the response of detector. After that, we bring the gold standard to LHO and calibrate the working standard Hanford, Livingston and KAGRA. The uncertainty of laser standard institutes is a few percent. The reduction of these uncertainties are essential for the gravitational wave observation.

3. GRAVITY FIELD CALIBRATOR

To solve the uncertainty problem of the absolute calibration, we propose the gravity field calibrator. The gravity field calibrator generate the gravity field at the end of test mass by rotating the multipole masses. The rotor placed in the vacuum chamber for isolating the acoustic noise. To monitor the frequency, we mount the 10-bit

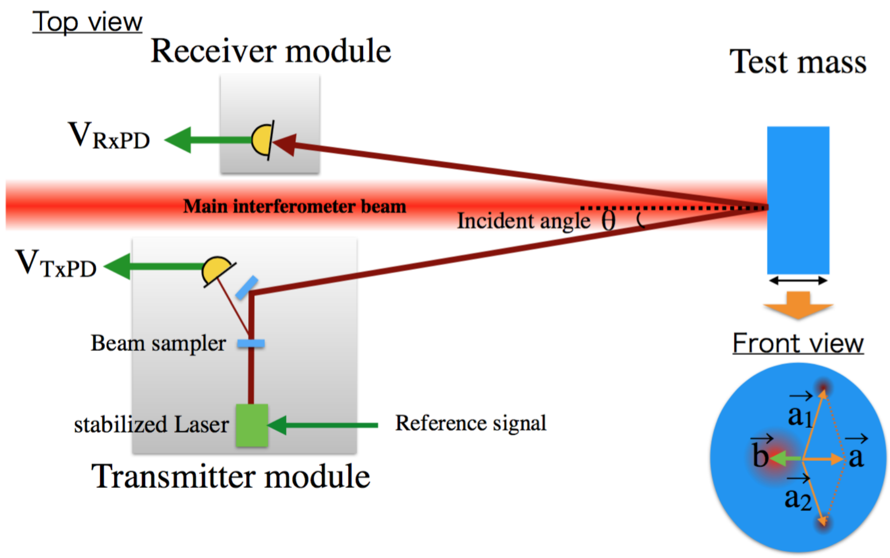

Figure 1. Schematic view of photon calibrator. We place the stabilized laser on the transmitter module. The injected signal at the test masses is monitored by using the responces of photo detector power between the transmitter module, V_{TxPD} and receiver module, V_{RxPD}. The geometrical factor is characterized by the position vectors of photon calibrator beams, $\vec{a} = \vec{a_1} + \vec{a_2}$, and the main beam, $\vec{b}$.

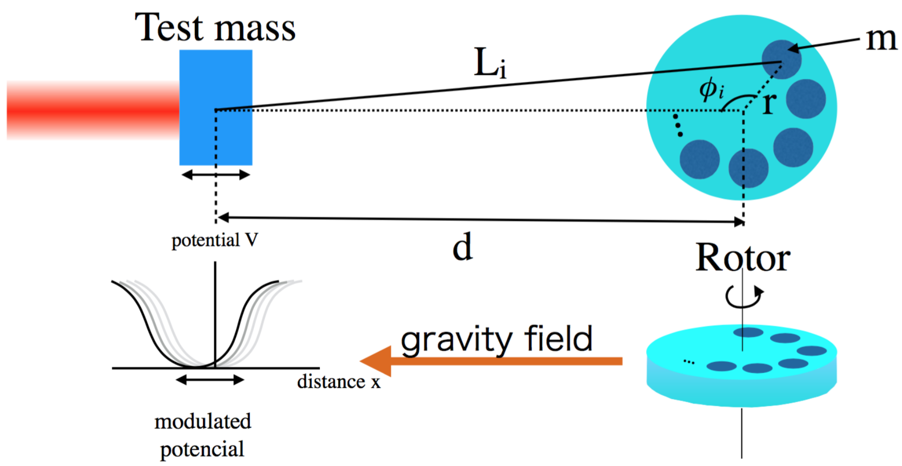

Figure 2. Schematic view of gravity field calibrator. We placed the rotor at the displacement of d away from test masses. Multipole mass generate the gravitational potential at the test mass position.

encoder. We monitor the frequency using 16 bit ADC system. We calculated the displacement by changing dynamic gravity field of multipole moment with with N masses. We assumed the suspended test mass for the interferometer and disk with multipole mass as shown in Fig ??. We put the masses m at the positions of the radius r. The distance between the center of mass of mirror and disk is assumed d. We rotate the disk at the angular frequency of $\omega_{rot} = 2\pi f_{rot}$.

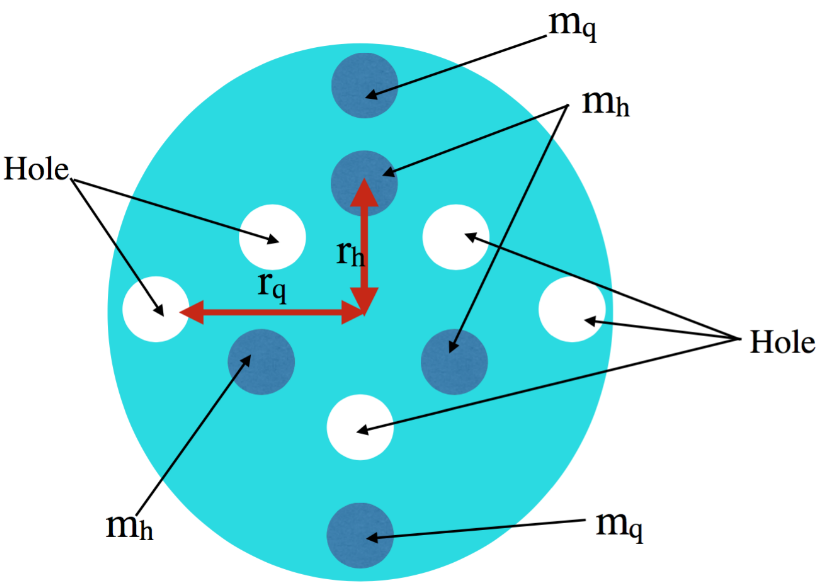

Figure 3. Configuration of the rotor with quadrupole and haxapole mass distribution. m_q and m_h are mass of quadrupole and hexapole. r_q and r_h are radius of quadrupole and hexapole.

Distance between i-th mass and center of test mass is written as

$$L_i = d\sqrt{1 + \left(\frac{r}{d}\right)^2 - 2\left(\frac{r}{d}\right)\cos\phi_i}, \tag{2}$$

where the angle of i-th mass is assumed as $\phi_i = \omega_{rot}t + 2\pi i/N$. The gravity potential at the center of test mass can be described as

$$\begin{aligned} V &= \Sigma_{i=0}^{N} V_i & (3)\\ &= -\frac{GMm}{d}\Sigma_{i=0}^{N}\Sigma_{n=0}^{\infty}\left(\frac{r}{d}\right)^n P_n\left(\cos\left(\omega_{rot}t + \frac{2\pi i}{N}\right)\right), & (4) \end{aligned}$$

where P_n is Legendre polynomial. The equation of motion of test mass is

$$Ma = \left|\frac{\partial V}{\partial d}\right| = \frac{GMm}{d^2}\Sigma_{i=0}^{N}\Sigma_{n=0}^{\infty}(n+1)\left(\frac{r}{d}\right)^n P_n\left(\cos\left(\omega_{rot}t + \frac{2\pi i}{N}\right)\right), \tag{5}$$

where a is acceleration of test mass. We place the quadrupole and hexapole masses in the same rotor as shown in Fig. **??**. We put the hole between each mass. The hole can increase the gravity gradient twice effectively. Therefore, we can describe the equation of motion as

$$Ma = \left|\frac{\partial V}{\partial d}\right| = \frac{2GMm}{d^2}\Sigma_{i=0}^{N}\Sigma_{n=0}^{\infty}(n+1)\left(\frac{r}{d}\right)^n P_n\left(\cos\left(\omega_{rot}t + \frac{2\pi i}{N}\right)\right). \tag{6}$$

We will calculate the displacement of quadrupole and hexapole in the section **??** and **??**.

3.1 Displacement of test mass (Quadrupole)

We calculate the displacement of the quadrupole mass distribution corresponding to $N = 2$. The masses and radiuses of quadrupole are assumed as m_q and r_q. The equation of motion of test mass is described as

$$Ma = \frac{2GMm_q}{d^2}\Sigma_{n=0}^{\infty}(n+1)\left(\frac{r_q}{d}\right)^n\left(P_n\left(\cos\left(\omega_{rot}t\right)\right) + P_n\left(\cos\left(\omega_{rot}t + \pi\right)\right)\right). \tag{7}$$

If we assume $r \ll d$, the displacement of the time-dependent lower harmonics can be written by

$$x = \Sigma_{k=1}^{\infty} x_{k\mathrm{f}} \cos(k\omega_{rot}t) \sim x_{2\mathrm{f}} \cos(2\omega_{rot}t) = x_{2f} \cos\omega t, \tag{8}$$

where k is the number of the harmonics. The amplitude of 2-f rotation is described as

$$x_{2\mathrm{f}} = 9\frac{GMm_q r_q^2}{d^4} s(\omega). \tag{9}$$

3.2 Displacement of test mass (Haxapole)

We calculate the displacement of the hexapole mass distribution, which corresponds to $N = 3$. The masses and radiuses of hexapole are assumed as m_h and r_h. The equation of motion of test mass is described as

$$\begin{aligned} Ma &= \frac{2GMm_h}{d^2} \Sigma_{n=0}^{\infty} (n+1) \left(\frac{r_h}{d}\right)^n \\ &\times \left(P_n \left(\cos\left(\omega_{rot}t\right)\right) + P_n \left(\cos\left(\omega_{rot}t + \frac{2\pi}{3}\right)\right) + P_n \left(\cos\left(\omega_{rot}t \frac{4\pi}{3}\right)\right)\right). \end{aligned} \tag{10}$$

If we assume $r \ll d$, the displacement of the time-dependent lower harmonics can be written by

$$x = \Sigma_{k=1}^{\infty} x_{k\mathrm{f}} \cos(k\omega_{rot}t) \sim x_{3\mathrm{f}} \cos(3\omega_{rot}t) = x_{3f} \cos\omega t, \tag{11}$$

where amplitude of 3-f is described as

$$x_{3\mathrm{f}} = 15\frac{GMm_h r_h^3}{d^5} s(\omega). \tag{12}$$

4. ABSOLUTE POWER CALIBRATION BY USING GCAL AND PCAL

In this section, we will discuss about absolute laser power calibration using interferometer. Figure **??** shows the configuration of the calibration by using the combination of photon calibrator and gravity field calibrator. First, we modulate the mirror position using gravity field calibrator. We can measure the signal of x_{2f} and x_{3f} in the response o interferometer. Second, we send the interferometer signal to the excitation port of photon calibrator as a reference of feedback control. The photon calibrator cancel the displacement by gravity field calibrator. Third, we measure the response of the detector of transmitter module and receiver module, whose unit is volt. The output signal of transmitter module, V_{TxPD} and receiver module, V_{RxPD} should be corresponding to displacement from gravity field. By using Eq (**??**),(**??**), and (**??**), the modulated powers are

$$P_{2f} = 18\frac{Gcm_q M r_q^2}{d^4 cos\theta} \frac{1}{1 + \frac{M}{I}\vec{a}\cdot\vec{b}} \tag{13}$$

$$P_{3f} = 30\frac{Gcm_h M r_h^3}{d^5 cos\theta} \frac{1}{1 + \frac{M}{I}\vec{a}\cdot\vec{b}} \tag{14}$$

Fourth, we demodulate the signal of transmitter and receiver module using the encoder signal of gravity field calibrator. The demodulated signals are

$$V_{2f}^T = \rho_T P_{2f} \tag{15}$$

$$V_{2f}^R = \rho_R P_{2f} \tag{16}$$

$$V_{3f}^T = \rho_T P_{3f} \tag{17}$$

$$V_{3f}^R = \rho_R P_{3f} \tag{18}$$

Therefore, we can calculate the distance with the ratio of response between 2-f and 3-f components:

$$d = \frac{5}{3}\frac{V_{2f}^T}{V_{3f}^T}\frac{m_h}{m_q}\frac{r_h^3}{r_q^2} = \frac{5}{3}\frac{V_{2f}^R}{V_{3f}^R}\frac{m_h}{m_q}\frac{r_h^3}{r_q^2}. \tag{19}$$

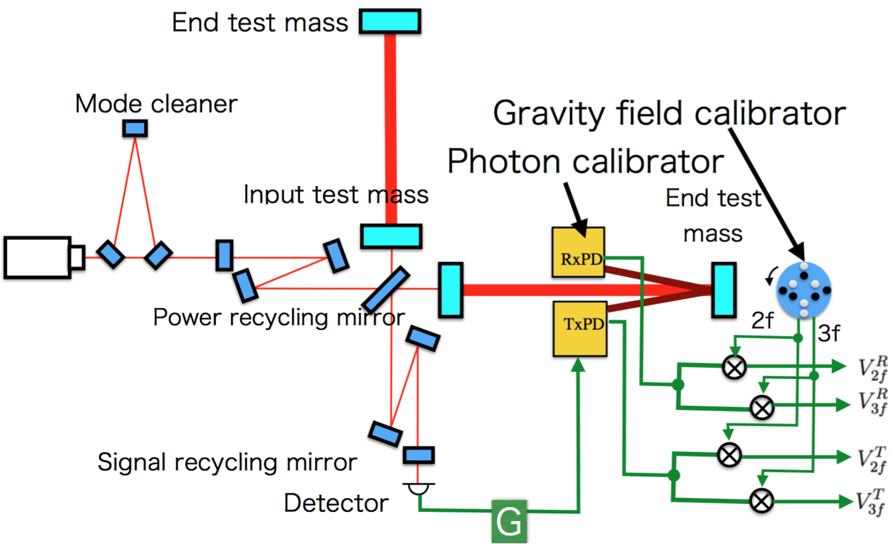

Figure 4. Test setup of the calibration of the laser power by rotating gravity field calibrator.

Table 2. The assumed parameters.

		Value	Relative uncertainty
G	Gravity constant	6.6742×10^{-11}	0.015 %
c	speed of light	2.99792458×10^8 [m/sec]	-
$\cos\theta$	Incident angle	$\cos 0.7[deg]$	0.07%
M	Mass of test mass	22.89 [kg]	0.02 %
m_q	Mass of quadrupole	4.485[kg]	0.004 %
m_h	Mass of hexapole	4.485[kg]	0.004%
r_q	Radius of quadrupole	0.200[m]	0.01 %
r_h	Radius of hexapole	0.125[m]	0.02%
$1+\frac{I}{M}\vec{a}\cdot\vec{b}$	Geometrical factor	1	0.3 %

Finally, we insert the equatin (**??**) to the Eq. (**??**):

$$x = \frac{P(\omega)\cos\theta}{2c}s(\omega)\left(1+\frac{M}{I}\vec{a}\cdot\vec{b}\right) \tag{20}$$

$$= 9\frac{P(\omega)}{P_{2f}}\frac{Gm_qMr_q^2}{d^4}s(\omega), \tag{21}$$

$$= \frac{729}{625}\frac{Gm_q^5r_q^{10}}{m_h^4r_h^{12}\omega^2}\frac{V_{3f}^{R\,4}}{V_{2f}^{R\,5}}V_0^R\cos\omega t, \tag{22}$$

where we assume $P(\omega) = \rho_R V_0^R\cos\omega t$, and V_0^R is amplitude of input voltage of the calibration line.

5. ESTIMATION OF UNCERTAINTY

In this section, we discuss the systematic error by changing the operation frequency and distance. After that, we discuss the uncertainty of the displacement of the mirror. We estimate the uncertainty of the displacement by assuming KAGRA basic parameter as shown in Fig. **??**. The assumed parameters of the calibrators are listed in Table **??**. We assumed these number in the following section.

5.1 Systematic error of the higher order term

In order to achieve the precision less than 1 %, we need to consider the operation position due to the higher order of Legendre polynomial. This is because that higher order also include the 2-f and 3-f components. The

Table 3. The calculated quadrupole($N = 2$) displacement. n is order of Legendre polynomial, where $\omega = n\omega_{rot}$.

modulation	n=1	n=2	n=3	n=4	n=5	n=6	n=7
1f	0	0	0	0	0	0	0
2f	0	$9\frac{Gmr^2}{d^4\omega^2}$	0	$\frac{25}{4}\frac{Gmr^4}{d^6\omega^2}$	0	$\frac{735}{128}\frac{Gmr^6}{d^8\omega^2}$	0
3f	0	0	0	0	0	0	0
4f	0	0	0	$\frac{175}{16}\frac{Gmr^4}{d^6\omega^2}$	0	$\frac{441}{64}\frac{Gmr^6}{d^8\omega^2}$	0
5f	0	0	0	0	0	0	0
6f	0	0	0	0	0	$\frac{1617}{128}\frac{Gmr^6}{d^8\omega^2}$	0

Table 4. The calculated hexapole($N = 3$) displacement. n is order of Legendre polynomial, where $\omega = n\omega_{rot}$.

modulation	n=1	n=2	n=3	n=4	n=5	n=6	n=7
1f	0	0	0	0	0	0	0
2f	0	0	0	0	0	0	0
3f	0	0	$15\frac{Gmr^3}{d^5\omega^2}$	0	$\frac{315}{32}\frac{Gmr^5}{d^7\omega^2}$	0	
4f	0	0	0	0	0	0	0
5f	0	0	0	0	0	0	0
6f	0	0	0	0	0	$\frac{4851}{256}\frac{Gmr^6}{d^8\omega^2}$	0

order of the Legendre polynomial is characterized by n as shown in Eq.(**??**). The effect of higher order factor is mitigated by the factor of $(r/d)^n$. Table **??** and **??** shows the calculated displacement of the higher order term. To compare the higher order effect, we calculate the ratio between the FEM and calculation by changing the r/d is shown in Fig **??**. We need to place the mirror at least 2m away from the mirror to reduce the systematic error. In the following calculation, we assume the distance as 2 m.

5.2 Systematic error of the transfer function

The gravity field calibrator can modulate the mirrors with gradient of gravity potential. However, its gravity gradient act the masses of suspension system as shown in Fig. **??**. We simulated the transfer function between

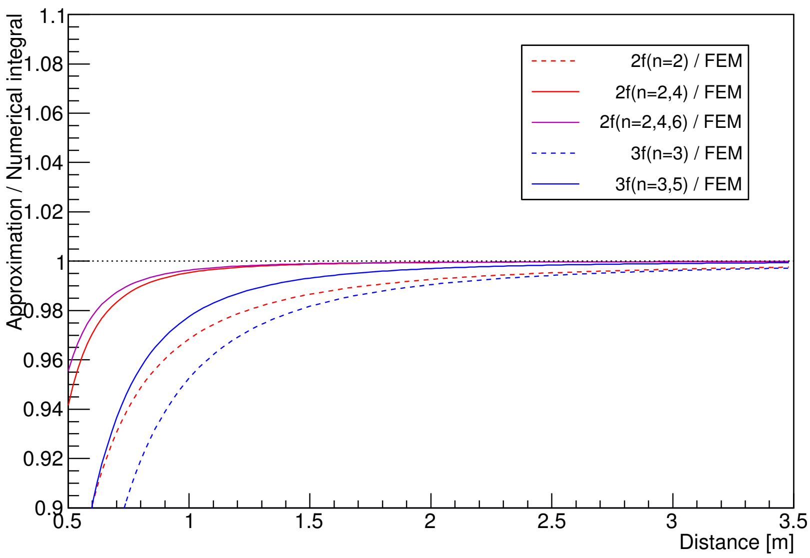

Figure 5. The displacement ratio of the higher order effect by changing r/d. Dashed curves are included with the 1st order term. Solid curves are included with sum of 1st order and 2nd order. The analytical result is listed in Table **??** and **??**. To achieve the precision less than 1%, we need include the higher order terms.

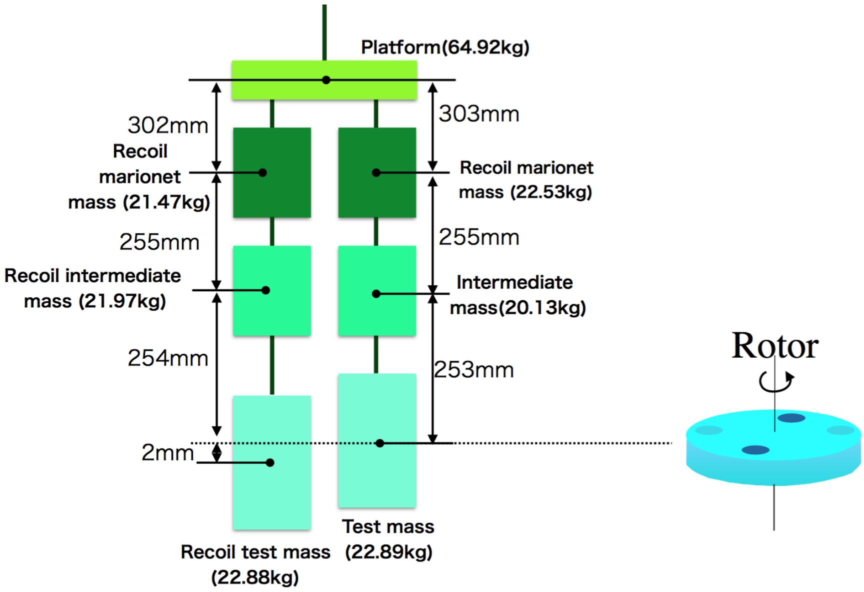

Figure 6. Schematic view of the suspension system. The parameter of the hight and mass is the assumed value.

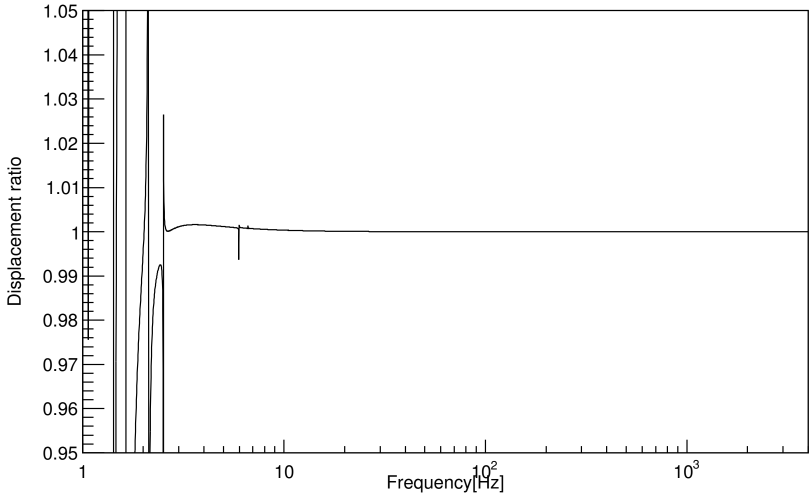

Figure 7. The displacement ratio of the transfer function of multi pendulum by changing modulation frequency, where relations of the modulation frequency, f, modulation angular frequency, ω, and rotation angular frequency, ω_{rot} are described as. $n\omega_{rot} = \omega = 2\pi f$. If we put the gravity field calibrator, it act the upper masses and it makes systematic error of the transfer function.

each mass and test mass. When we calculate the transfer function, we used a code of SUMCOM based on mathematica. We estimated the total displacement including all the masses. Figure **??** shows the displacement ratio between the sensed motion and free mass motion as a function of frequency The structures of low frequency are corresponding to the resonant peak of the suspension system. We can neglect the intermediate mass effect and regard as free mass motion larger than 10 Hz. We assumed the rotation frequency as 16 Hz, which is corresponding to 32 Hz and 48Hz at the operation frequency. of 2-f and 3-f components. We used this assumption in the following section.

5.3 Uncertainty of displacement and laser power

In this section, we estimate the typical displacement based on the Table. ??. The estimated displacements of 2f and 3f are described as

$$\begin{aligned} x_{2f}^{rms} &= 1.178\times 10^{-16}[\mathrm{m}] \times \left(\frac{G}{6.6742\times 10^{-11}[\mathrm{m^3kg^{-1}sec^{-2}}]}\right) \times \left(\frac{m_q}{4.485[\mathrm{kg}]}\right) \times \left(\frac{r_q}{0.200[\mathrm{m}]}\right)^2 \\ &\times \left(\frac{2[\mathrm{m}]}{d}\right)^4 \times \left(\frac{2\pi(2\times 16)[\mathrm{Hz}]}{\omega}\right)^2 \end{aligned} \quad (23)$$

$$\begin{aligned} x_{3f}^{rms} &= 2.130\times 10^{-18}[\mathrm{m}] \times \left(\frac{G}{6.6742\times 10^{-11}[\mathrm{m^3kg^{-1}sec^{-2}}]}\right) \times \left(\frac{m_h}{4.485[\mathrm{kg}]}\right) \times \left(\frac{r_h}{0.125[\mathrm{m}]}\right)^3 \\ &\times \left(\frac{2[\mathrm{m}]}{d}\right)^5 \times \left(\frac{2\pi(3\times 16)[\mathrm{Hz}]}{\omega}\right)^2. \end{aligned} \quad (24)$$

This displacement is much higher than the sensitivity of KAGRA. By using this result, we estimate the signal to noise ratio of the peaks.

$$SNR_{2f} = 392 \times \left(\frac{3.0\times 10^{-19}\mathrm{m}/\sqrt{\mathrm{Hz}}}{n_{32Hz}}\right) \times \left(\frac{T}{1[\mathrm{sec}]}\right)^{1/2} \times \left(\frac{x_{2f}^{rms}}{1.178\times 10^{-16}[m]}\right) \quad (25)$$

$$SNR_{3f} = 73 \times \left(\frac{2.9\times 10^{-20}\mathrm{m}/\sqrt{\mathrm{Hz}}}{n_{48Hz}}\right) \times \left(\frac{T}{1[\mathrm{sec}]}\right)^{1/2} \times \left(\frac{x_{2f}^{rms}}{2.130\times 10^{-18}[m]}\right) \quad (26)$$

$$(27)$$

We can apply this system for the measurement of the absolute laser power. The estimated powers are

$$\begin{aligned} P_{2f} &= 0.09288\ [\mathrm{W}] \times \left(\frac{G}{6.6742\times 10^{-11}[\mathrm{m^3kg^{-1}sec^{-2}}]}\right) \times \left(\frac{c}{2.99792458\times 10^{8}[\mathrm{msec^{-1}}]}\right) \\ &\times \left(\frac{m_q}{4.485[\mathrm{kg}]}\right) \times \left(\frac{r_q}{0.200[\mathrm{m}]}\right)^2 \times \left(\frac{2[\mathrm{m}]}{d}\right)^4 \times \left(\frac{1}{\cos\theta}\right) \times \left(\frac{1}{1+\frac{M}{I}\vec{a}\cdot\vec{b}}\right)^2 \end{aligned} \quad (28)$$

$$\begin{aligned} P_{3f} &= 0.003779\ [\mathrm{W}] \times \left(\frac{G}{6.6742\times 10^{-11}[\mathrm{m^3kg^{-1}sec^{-2}}]}\right) \times \left(\frac{c}{2.99792458\times 10^{8}[\mathrm{msec^{-1}}]}\right) \\ &\times \left(\frac{m_h}{4.485[\mathrm{kg}]}\right) \times \left(\frac{r_h}{0.125[\mathrm{m}]}\right)^3 \times \left(\frac{2[\mathrm{m}]}{d}\right)^5 \times \left(\frac{1}{\cos\theta}\right) \times \left(\frac{1}{1+\frac{M}{I}\vec{a}\cdot\vec{b}}\right)^2. \end{aligned} \quad (29)$$

The estimated V_{2f}^T/V_{3f}^T by changing distance are shown in Fig. ??.

The uncertainty of the quadrupole and hexapole masses are limited by the accuracy of electronic balance. In this case, we use the weight made of Tungsten. The density of Tungsten is 19.25 g/cm^3. The diameter and thickness of mass are 0.06m and 0.08 m, respectively. Therefore, the mass of the rotor mass is 4.485 kg. To measure this mass, we assumed that we use an electronic balance whose catalog number and accuracy are CG-6000 and 0.2 g, respectively. Therefore, the relative uncertainty of the mass of rotor mass is 0.04 %.

To make the rotor disk, we use the NC milling machine. The typical accuracy is less than 0.02 mm. For the measuring of the shape, we employ the three-dimension coordinate measuring machine (CMM).[?] The precision of CMM is 2 μm. We can measure the shape of the rotor and masses with enough of uncertainty using CMM.

The estimated relative uncertainty of displacement is written as

$$\begin{aligned} \left(\frac{\delta x}{x}\right)^2 &\sim \left(\frac{\delta G}{G}\right)^2 + \left(\frac{\delta V_0^R}{V_0^R}\right)^2 + 4\left(\frac{\delta\omega}{\omega}\right)^2 + 25\left(\frac{\delta m_q}{m_q}\right)^2 + 16\left(\frac{\delta m_h}{m_h}\right)^2 \\ &+ 25\left(\frac{\delta V_{f2}^R}{V_{f2}^R}\right)^2 + 16\left(\frac{\delta V_{f3}^R}{V_{f3}^R}\right)^2 + 100\left(\frac{\delta r_q}{r_q}\right)^2 + 144\left(\frac{\delta r_h}{r_h}\right)^2. \end{aligned} \quad (30)$$

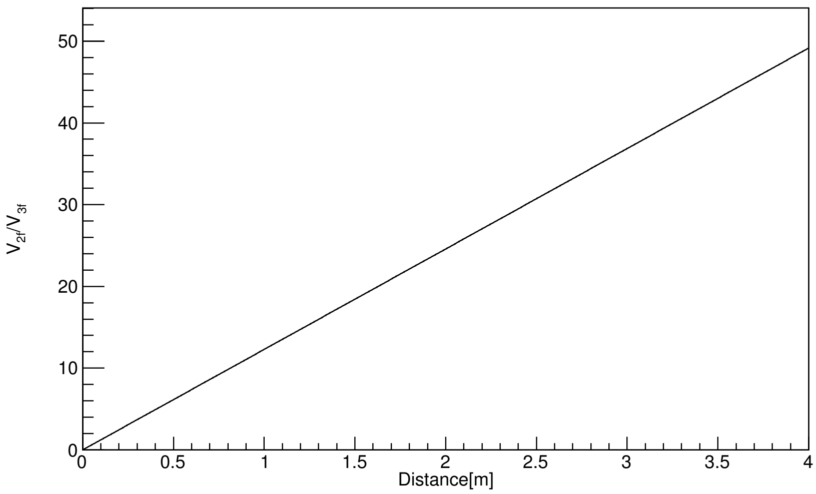

Figure 8. The response of V_{2f}/V_{3f} by changing distance between test mass and gravity field calibrator.

The contribution of the radius uncertainty is amplified by the O(100) factor. To reduce the noise of displacement, we need to reduce the uncertainty of the shape of the rotor and masses. The uncertainty of the V_{2f}^R,V_{3f}^R, V_0^R are much less than other contributions.We can reduce the uncertainty of these values with long time integration time due to the statistics. Each the uncertainty is listed in Table. **??**. The estimated total uncertainty of the displacement is 0.3 %.

We can also estimate the laser power by using the following equations:

$$\begin{aligned}\left(\frac{\delta P_{2f}}{P_{2f}}\right)^2 &\sim \left(\frac{\delta G}{G}\right)^2 + \left(\frac{\delta c}{c}\right)^2 + \left(\frac{\delta M}{M}\right)^2 + 25\left(\frac{\delta m_q}{m_q}\right)^2 + 16\left(\frac{\delta m_h}{m_h}\right)^2 + 100\left(\frac{\delta r_q}{r_q}\right)^2 + 144\left(\frac{\delta r_h}{r_h}\right)^2 \\ &+ 16\left(\frac{\delta V_{f2}^R}{V_{f2}^R}\right)^2 + 16\left(\frac{\delta V_{f3}^R}{V_{f3}^R}\right)^2 + \left(\frac{\delta(\cos\theta)}{\cos\theta}\right)^2 + \left(\frac{\delta\left(1+\frac{M}{I}\vec{a}\cdot\vec{b}\right)}{\left(1+\frac{M}{I}\vec{a}\cdot\vec{b}\right)}\right)^2 \end{aligned} \tag{31}$$

$$\begin{aligned}\left(\frac{\delta P_{3f}}{P_{3f}}\right)^2 &\sim \left(\frac{\delta G}{G}\right)^2 + \left(\frac{\delta c}{c}\right)^2 + \left(\frac{\delta M}{M}\right)^2 + 25\left(\frac{\delta m_q}{m_q}\right)^2 + 16\left(\frac{\delta m_h}{m_h}\right)^2 + 100\left(\frac{\delta r_q}{r_q}\right)^2 + 144\left(\frac{\delta r_h}{r_h}\right)^2 \\ &+ 16\left(\frac{\delta V_{f2}^R}{V_{f2}^R}\right)^2 + 16\left(\frac{\delta V_{f3}^R}{V_{f3}^R}\right)^2 + \left(\frac{\delta(\cos\theta)}{\cos\theta}\right)^2 + \left(\frac{\delta\left(1+\frac{M}{I}\vec{a}\cdot\vec{b}\right)}{\left(1+\frac{M}{I}\vec{a}\cdot\vec{b}\right)}\right)^2 \end{aligned} \tag{32}$$

The estimated relative uncertainties of the powers are 0.4%. One of the largest uncertainty is the geometrical factor of the Pcal laser. The geometrical factor uncertainty is assumed 0.3 %, which is same number of LIGO.

6. CONCLUSION

Photon calibrator is one of the powerful calibrators in advanced LIGO, advanced Virgo and KAGRA. It can calibrate the response of IFO and its uncertainty is essential for estimation of gravitational wave source. In particular, the distance of the source is strongly depend on the absolute laser power of the photon calibrator. In previous study, the Gold standard, which response is calibrated by the laser power standard of NIST, is used for the absolute laser power calibration of the photon calibrator. However, current limit of the absolute laser power between each country is about 3 %. It is directly propagate to the uncertainty of absolute displacement of gravitational wave detector.

To solve the problem, we proposed the combination method of photon calibrator and gravity field calibrator. Gravity field calibrator can modulate the mirror using gravity gradient. By canceling the displacement of the test mass using the photon calibrator, we can calibrate the absolute laser power and displacement of the photon calibrator with accuracy of 0.4 % and 0.3%.

This method has an advantage of a direct comparison of the amplitude of injected power and gravity field. In previous study, we need to consider the uncertainty of the optical efficiency through the window and mirrors. This is because we put the working standard at the outside of the chamber. However, the method of gravity field can compare the displacement directly. By using this method, we can calibrate the uncertainty of optical efficiency and absolute power of the laser. When we compare the laser power between each institute, we need to bring the working standard. However, we can try the absolute calibration using this method. As we mention about a few percent of the absolute uncertainty of laser in each country. The estimated uncertainty of the power of this method is 0.4%. It imply that we can make a new power standard using interferometer.

ACKNOWLEDGMENTS

We thank Rechard Savage, Darkhan Tuyrnbayev for diskussion of the photon calibrator. We would like to express our gratitude to Prof.Takaaki Kajita and Prof.Henry Wong. We would like to thank the KEK Cryogenics Science Center for the support. YI was supported by Academia Sinica under Grants No. CDA-105-M06 in Taiwan. This work was supported by JSPS KAKENHI Grant Numbers XXXXXX and XXXXXX, and by the JSPS Core-to-Core Program.

REFERENCES

[1] Abbott, B. P. et al., "Observation of gravitational waves from a binary black hole merger," *Phys. Rev. Lett.* **116**, 061102 (Feb 2016).

[2] Acernese, F. et al., "Advanced virgo: a second-generation interferometric gravitational wave detector," *Classical and Quantum Gravity* **32**(2), 024001 (2015).

[3] Somiya, K., "Detector configuration of kagra–the japanese cryogenic gravitational-wave detector," *Classical and Quantum Gravity* **29**(12), 124007 (2012).

[4] Aso, Y., Michimura, Y., Somiya, K., Ando, M., Miyakawa, O., Sekiguchi, T., Tatsumi, D., and Yamamoto, H., "Interferometer design of the kagra gravitational wave detector," *Phys. Rev. D* **88**, 043007 (Aug 2013).

[5] Karki, S., Tuyenbayev, D., Kandhasamy, S., Abbott, B. P., Abbott, T. D., Anders, E. H., Berliner, J., Betzwieser, J., Cahillane, C., Canete, L., Conley, C., Daveloza, H. P., Lillo, N. D., Gleason, J. R., Goetz, E., Izumi, K., Kissel, J. S., Mendell, G., Quetschke, V., Rodruck, M., Sachdev, S., Sadecki, T., Schwinberg, P. B., Sottile, A., Wade, M., Weinstein, A. J., West, M., and Savage, R. L., "The advanced ligo photon calibrators," *Review of Scientific Instruments* **87**(11), 114503 (2016).

[6] Matone, L., Raffai, P., Márka, S., Grossman, R., Kalmus, P., Márka, Z., Rollins, J., and Sannibale, V., "Benefits of artificially generated gravity gradients for interferometric gravitational-wave detectors," *Classical and Quantum Gravity* **24**(9), 2217 (2007).

[7] Tuyenbayev, D., Karki, S., Betzwieser, J., Cahillane, C., Goetz, E., Izumi, K., Kandhasamy, S., Kissel, J. S., Mendell, G., Wade, M., Weinstein, A. J., and Savage, R. L., "Improving ligo calibration accuracy by tracking and compensating for slow temporal variations," *Classical and Quantum Gravity* **34**(1), 015002 (2017).

[8] Inoue, Y. et al., "Two-layer anti-reflection coating with mullite and polyimide foam for large-diameter cryogenic infrared filters," (2016). [Appl. Opt.55,22(2016)].